Scattering of near-zero-energy electrons and positrons by H_2

J.-Y. Zhang,[1,*] Y.-J. Yang,[2] Y. Qian,[3] Z.-C. Yan,[4,5] and U. Schwingenschlögl[1,†]

[1]*PSE Division, King Abdullah University of Science and Technology, Thuwal 23955-6900, Saudi Arabia*

[2]*Institute of Atomic and Molecular Physics, Jilin University, Changchun 130012, China*

[3]*Department of Computer Science and Technology, East China Normal University, Shanghai, China*

[4]*Department of Physics, University of New Brunswick, Fredericton, New Brunswick, Canada E3B 5A3*

[5]*State Key Laboratory of Magnetic Resonance and Atomic and Molecular Physics, Wuhan Institute of Physics and Mathematics, and Center for Cold Atom Physics, Chinese Academy of Sciences, Wuhan 430071, China*

(Received 25 December 2013; published 15 April 2014)

The parameters for S-wave elastic scattering of near-zero-energy electrons and positrons by H_2 molecules are calculated using the stabilization method with explicitly correlated Gaussians. The confined variational method is applied to optimize the Gaussians to describe the short-range interaction of incident $e^{\pm}$ with H_2 in the fixed-nuclei approximation. For e^+-H_2 scattering the scattering length of previous work [Phys. Rev. Lett. **103**, 223202 (2009)] is substantially improved. More importantly, for e^--H_2 scattering, from first principles, the scattering length is computed as a function of the internuclear distance. In the case that the two nuclei are at the equilibrium distance the results are in a good agreement with values derived from fitting experimental total and diffusion cross sections to the modified effective range theory.

DOI: 10.1103/PhysRevA.89.042703 PACS number(s): 34.80.Bm, 34.10.+x, 03.65.Nk, 34.80.Uv

I. INTRODUCTION

The scattering of $e^{\pm}$ from H_2 is of fundamental interest and has been the subject of intensive theoretical and experimental investigations for decades [1–23]. Due to the dual-center nature of molecular H_2, theoretical calculations for the low-energy $e^{\pm}$ scattering are much more challenging than for the scattering by He atoms. Hence there exist few well-converged first-principles calculations, even for H_2 in the fixed-nuclei approximation. In the case of low-energy scattering, the incident $e^{\pm}$ can interact with the target for a relatively long period of time before moving away. Therefore, the scattering depends significantly on the complicated correlation interaction with the target.

In this work, the low-energy $e^{\pm}$-H_2 scattering is studied using the stabilization method [24,25] in the fixed-nuclei approximation. Explicitly correlated Gaussians (ECGs) [26–28] are chosen as basis functions, which have the advantage that the Hamiltonian matrix elements of the scattering system can be evaluated analytically. To improve the description of the complicated short-range interaction, the confined variational method is adopted to optimize the ECGs. The idea of adding a confining potential to the Hamiltonian previously has been used to study $e^{\pm}$ and positronium scattering [29–32]. For the e^+-H_2 scattering, the scattering lengths of previous ECG calculations [32] can be significantly improved by larger basis sets, by optimizing the energy of the lowest pseudostate for each confined system rather than optimizing the mean energy of the lowest two pseudostates, and by taking into account the polarization correction. For the e^--H_2 scattering, our present scattering length of $1.24a_0$ is in good agreement with the values obtained by the modified effective range theory (MERT), $A_{\rm scat} = 1.27 \pm 0.01a_0$ [33,34], $1.29a_0$ [35], and $1.30a_0$ [23].

*Junyi.Zhang@kaust.edu.sa

†Udo.Schwingenschlogl@kaust.edu.sa

II. THEORY AND COMPUTATIONAL METHOD

Atomic units are used throughout this paper. The Hamiltonian for $e^{\pm}$-H_2 scattering is

$$H = -\sum_{i=1}^{3}\frac{\nabla_i^2}{2} + \sum_{j>i=1}^{3}\frac{q_i\,q_j}{|\mathbf{r}_j - \mathbf{r}_i|} + \sum_{i=1}^{3}\left\{\frac{q_i}{|\mathbf{r}_i - \mathbf{R}/2|} + \frac{q_i}{|\mathbf{r}_i + \mathbf{R}/2|}\right\}, \quad (1)$$

where $\mathbf{r}_i$ is the coordinate of the ith light particle (electron or positron) relative to the midpoint of the internuclear axis, q_i is the corresponding charge, and $\pm\mathbf{R}/2$ represents the displacement of the two protons, respectively, from the midpoint. The basis functions for the interaction region have the form

$$\phi_k = \hat{P}\,\exp\left(-\frac{1}{2}\sum_{i=1}^{3} b_{k,i}|\mathbf{r}_i - \mathbf{S}_{k,i}|^2\right) \times \exp\left(-\frac{1}{2}\sum_{i=1}^{2}\sum_{j=i+1}^{3} a_{k,ij}|\mathbf{r}_i - \mathbf{r}_j|^2\right). \quad (2)$$

The vector $\mathbf{S}_{k,i}$ displaces the center of the ECG for the ith particle to a point on the internuclear axis, ensuring that the wave function is of Σ symmetry. The operator $\hat{P}$ forces the wave function to have Σ_g symmetry. Each ECG has a total of nine parameters $a_{k,ij}$, $b_{k,i}$, and $\mathbf{S}_{k,i}$, which are adjusted in the optimization process.

To improve the description of correlations between the incident $e^{\pm}$ and molecular electrons, a confining potential $W_{\rm CP}(r_i)$ for each lepton is added in the Hamiltonian, given by

$$W_{\rm CP}(r_i) = 0, \quad r_i < R_0, \quad (3)$$

$$W_{\rm CP}(r_i) = G(r_i - R_0)^2, \quad r_i \geqslant R_0, \quad (4)$$

where G is a small positive number, 1.55×10^{-4} for e^+ scattering and 6.0×10^{-5} for the e^- scattering. Moreover,

TABLE I. Convergence of calculations for the Σ_g e^+-H_2 system at $R = 1.4a_0$ with respect to the number of ECGs. Results for $R = 1.45a_0$, calculations by other groups, and experimental measurements are included. Energies $E_{N_{\text{inner}}}$, wave numbers k, and scattering lengths A_{scat} are given in atomic units.

$N_{\text{inner}} + N_{\text{outer}}$	$E_{N_{\text{inner}}}$	k	$A_{\text{scat},\parallel}$	$A_{\text{scat},\perp}$	$Z_{\text{eff},\parallel}$	$Z_{\text{eff},\perp}$
		$R = 1.4$				
$600 + 36$	$-1.169\,468\,17$	$0.635\,577 \times 10^{-2}$	-2.508	-2.763	14.37	14.59
$1000 + 36$	$-1.169\,470\,50$	$0.635\,547 \times 10^{-2}$	-2.496	-2.771	14.65	14.87
$1400 + 36$	$-1.169\,472\,07$	$0.635\,530 \times 10^{-2}$	-2.478	-2.793	14.62	14.88
$2600 + 36$	$-1.169\,472\,22$	$0.635\,511 \times 10^{-2}$	-2.450	-2.809	14.66	14.95
Mean value			-2.63		14.80	
Stabilization: ECG [32]	$-1.169\,461\,86$	$0.635\,551 \times 10^{-2}$	-2.53	-2.63	14.74	14.83
Kohn: ECG [40]			-2.565		14.61	
Kohn: Method of models [12,42,48]			-2.2		12.6	
Kohn: Method of models [42]		0.01	-2.56		13.5	
		$R = 1.45$				
$1600 + 36$	$-1.169\,089\,17$	$0.635\,264 \times 10^{-2}$	-2.594	-2.982	15.67	16.00
Mean value			-2.79		15.80	
Kohn: ECG [40]			-2.709		15.70	
MERT fit [23,44]			-2.51			
MERT fit [23,45]			-3.13			
Experiment, $k \approx 0.045a_0^{-1}$, $R \approx 1.448a_0$ [7]					14.7(2)	
Experiment, $k \approx 0.045a_0^{-1}$, $R \approx 1.448a_0$ [13]					14.61(14)	
Experiment, $k \approx 0.045a_0^{-1}$, $R \approx 1.448a_0$ [8]					16.02(08)	

R_0 must be larger than the interaction region in order to avoid disturbing the interaction between $e^{\pm}$ and target. We use $R_0 = 18a_0$ for all calculations presented in this article. By applying the confining potential, the continuum state problem is converted into a problem of discrete energy levels. Therefore, the basis set for the short-range interaction is optimized by minimizing the lowest energy of the confined system by the stochastic variational method [28,36,37].

To enlarge the basis, we merge several basis sets, each being well optimized for a specific interatomic distance. For e^+-H_2 scattering, for example, the basis sets for $R = 1.4$ and $1.6a_0$ are merged to form the basis set of the interaction region for $R = 1.4a_0$. As compared to e^+-H_2 scattering, for e^--H_2 scattering the optimization of the inner basis functions is much more time-consuming and difficult. Besides the more complicated permutation symmetry, the main reason is that the near-linear dependence frequently occurs when the size of the basis set is larger than 800. We again merge several well optimized basis sets for different interatomic distances. For example, the basis set of the interaction region for $R = 1.4a_0$ is composed of the basis sets for $R = 1.4$, 1.6, and $1.8a_0$. For some values of R the Schrödinger equation for the confined system cannot be solved with the merged basis set. However, in most cases a solution is possible when the confining potential is excluded. By adding a certain number of basis functions each time and trying to solve the Schrödinger equation without confining potential, we determine which basis functions cause the near-linear dependence. After a successful solution, we obtain the corresponding eigenenergies and eigenwave functions, which are orthonormalized to each other. The lowest eigenenergy, which is higher than the ground-state energy of fixed-nuclei H_2, becomes lower when the number of basis functions increases. Otherwise, the near-linear dependence occurs and the basis functions added in the last step must be removed. In addition, the quality of the finally selected inner basis functions is confirmed for mutual consistency by the convergence of the scattering parameters (see Tables I and II).

For scattering at very low energy, the convergence of the scattering parameters can be improved by including exterior basis sets to describe the asymptotic region, which are given by products of H_2 wave functions and Gaussians,

$$\Psi_{i,\text{outer}} = \psi^{H_2}(\mathbf{r}_1,\mathbf{r}_2)\exp\left(-\tfrac{1}{2}\alpha_i\mathbf{r}_3^2\right). \tag{5}$$

The H_2 wave functions for different distances R are represented by linear combinations of 100 or 120 ECGs. For example, the calculated ground-state energy of H_2 for $R = 1.40a_0$ is $-1.174\,475\,54$ hartree using a basis set of 120 ECGs, i.e., only 1.7×10^{-7} hartree higher than the close-to-exact value $-1.174\,475\,71$ hartree [38]. The Gaussians are introduced to represent the asymptotic behavior of the incident particle. Moreover, $\{\alpha_i\}$ is an even tempered set given by the relation $\alpha_i = \alpha_1/T^{i-1}$ with $\alpha_1 = 18.59$ and $T = 1.435$. A total of 36 long-range functions is added to each interaction region basis set.

The Hamiltonian matrices (excluding the confining potential) are constructed with both inner and exterior basis functions. Diagonalization leads to a set of eigenenergies and wave functions. In the stabilization method [24,25] eigenwave functions with positive energy are reasonable approximations to the exact scattering wave functions. The phase shifts are derived by a least-squares fit to the overlap of the target wave function and the wave function of the $e^{\pm}$-H_2 scattering. The overlap function

$$C(\mathbf{r}_3) = \int d^3r_1 d^3r_2 \psi^{H_2}(\mathbf{r}_1,\mathbf{r}_2)\Psi(\mathbf{r}_1,\mathbf{r}_2,\mathbf{r}_3) \tag{6}$$

depends on the distance r_3 of the incident $e^{\pm}$ from the internuclear midpoint and the angle θ_3 with respect to the internuclear axis.

TABLE II. Convergence of the calculations for the Σ_g e^--H_2 system at $R = 1.4a_0$ with respect to the number of ECGs. Energies $E_{N_{\text{inner}}}$, wave numbers k, and scattering lengths A_{scat} are given in atomic units.

$N_{\text{inner}} + N_{\text{outer}}$	$E_{N_{\text{inner}}}$	k	$A_{\text{scat},\parallel}$	$A_{\text{scat},\perp}$
$1000 + 36$	$-1.169\,430\,34$	$0.640\,734 \times 10^{-2}$	1.161	1.333
$1500 + 36$	$-1.169\,435\,11$	$0.640\,723 \times 10^{-2}$	1.149	1.338
$2000 + 36$	$-1.169\,435\,41$	$0.640\,715 \times 10^{-2}$	1.124	1.353
$2500 + 36$	$-1.169\,435\,60$	$0.640\,712 \times 10^{-2}$	1.118	1.355
Mean value			1.24	
MERT fit by Fedus and co-workers [23]			1.30	
MERT fit by Chang [33]			1.27 ± 0.01	
MERT fit by Fabrikant [35]			1.29	

During the scattering the $e^{\pm}$ experiences a long-range potential of which the dominating part is given by

$$V_{\text{LR}}(\mathbf{r}_3) \simeq -\frac{\alpha}{2r_3^4} - \frac{\alpha_2}{2r_3^4} P_2(\cos\theta_3) - \frac{Q}{2r_3^3} P_2(\cos\theta_3), \quad (7)$$

where α and α_2 are the isotropic and anisotropic polarizabilities of H_2, respectively [34]. $P_2(\cos\theta_3)$ is a Legendre polynomial of order two and the third term represents the quadrupole potential, Q being the quadrupole moment of H_2. For the scattering of near-zero-energy electrons by ground-state H_2 the S-wave elastic scattering dominates, while other channels as well as channel coupling effects of the orientation-dependent part of the long-range potential are negligible [39]. Thus the fixed-nuclei approximation is reasonable. The effect of isotropic potential on the phase shifts is taken into account by integrating the asymptotic form $B(\theta_3)\sin[kr_3 + \delta_k(\theta_3)]$ of the wave functions inward to the inner boundaries of the least-squares fits, which are made over the interval $[R_1, R_2]$ at fixed values of θ_3. The value of R_1 should be sufficiently large for the projectile and target wave functions to have minimal overlap, typically $R_1 = 15a_0$ for few-electron atomic and molecular targets. The value of R_2 should ensure that the probability density of the particle remains a reasonable fraction (e.g., 20%) of the peak probability density, typically $R_2 = 25$ to $30a_0$. In this work we chose $R_1 = 18a_0$ and $R_2 = 30a_0$. For the e^+-H_2 scattering the positrons may annihilate with the electrons of H_2 to create photons. The annihilation parameter Z_{eff}, which represents the effective number of electrons available for annihilation, is determined by the normalization constant $B(\theta_3)$.

III. RESULTS AND DISCUSSION

A. Near-zero-energy positron scattering from H_2

Table I addresses the convergence of the calculations for the Σ_g e^+-H_2 system at $R = 1.4a_0$ as a function of the number of ECGs, $N_{\text{inner}} + N_{\text{outer}}$, where N_{inner} is the number of inner region basis functions and N_{outer} is the number of outer region basis functions. The energy of the lowest state in the confining potential is given by the $E_{N_{\text{inner}}}$ column. The wave number k (in a_0^{-1}) refers to the lowest-energy pseudostate when the entire basis is diagonalized without confining potential. A_{scat} (in a_0) and Z_{eff} are derived from the wave-function projections parallel ($\parallel$) and perpendicular ($\perp$) to the internuclear axis. While we optimize the basis sets for the inner region by minimizing the energy of the lowest pseudostate, in previous ECG calculations [32,40] the mean energy of the two lowest pseudostates has been minimized during the optimization. In addition, since the size of the present basis sets is larger and the polarization effect of H_2 is taken into account, improved results can be expected.

As the number of basis functions increases, $E_{N_{\text{inner}}}$, k, A_{scat}, and Z_{eff} change monotonically; see Table I. The inner basis set is optimized for $R = 1.4a_0$ up to a size of 1400. For calculating the scattering parameters with the stabilization method 1200 basis functions optimized for $R = 1.6a_0$ are added, which improves the results by about 0.5% to 1% though the corresponding $E_{N_{\text{inner}}}$ is just slightly lower than for 1400 basis functions. As compared to the previous ECG calculation in Ref. [32], our $A_{\text{scat},\parallel}$ is 3% larger and our $A_{\text{scat},\perp}$ is 7% smaller. As expected, the difference between these two quantities grows when the number of basis functions increases. Armour and co-workers have calculated A_{scat} and Z_{eff} by the Kohn variational method [41–43]. Their phase shift for $k = 0.01a_0^{-1}$ gives a scattering length of $-2.56a_0$ [42]. Fedus and co-workers have obtained MERT scattering lengths of $-2.51a_0$ and $-3.13a_0$ [23] by fitting the experimental data of Hoffmann and co-workers [44] and Karwasz and co-workers [45], respectively. The fit values are close to the limits of our $A_{\text{scat},\parallel}$ and $A_{\text{scat},\perp}$ for $R = 1.45a_0$ (i.e., almost the equilibrium distance $1.448a_0$). The experimental $Z_{\text{eff}} = 14.7$ [7], 16.02 [8],

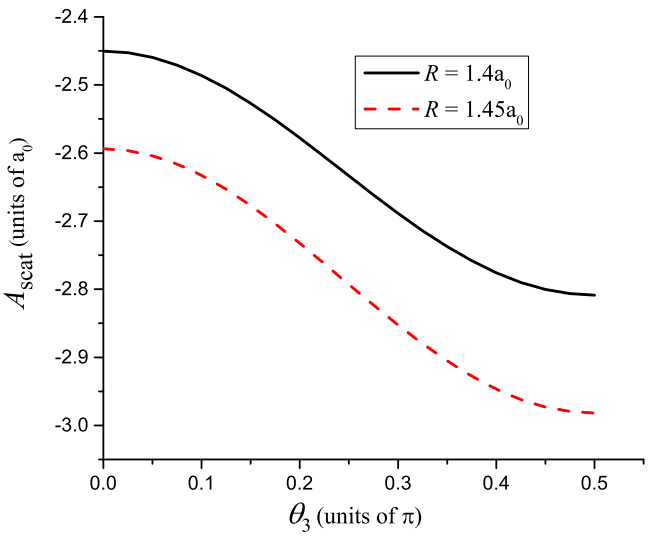

FIG. 1. (Color online) Scattering length A_{scat} as a function of the angle θ_3 for e^+-H_2 scattering.

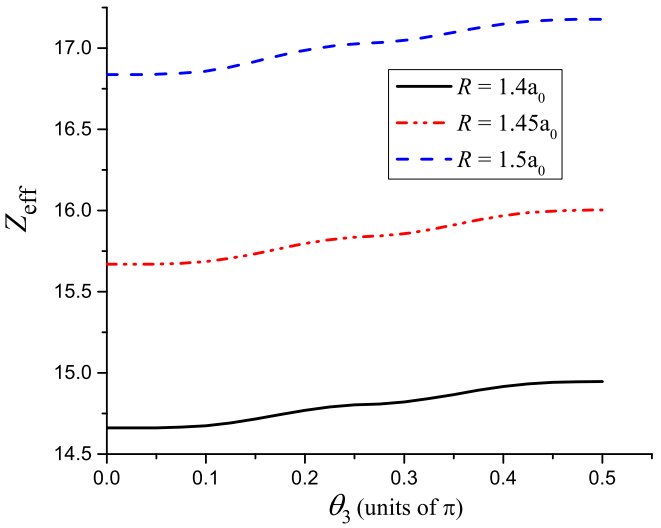

FIG. 2. (Color online) Annihilation parameter Z_{eff} as a function of the angle θ_3 for e^+-H_2 scattering.

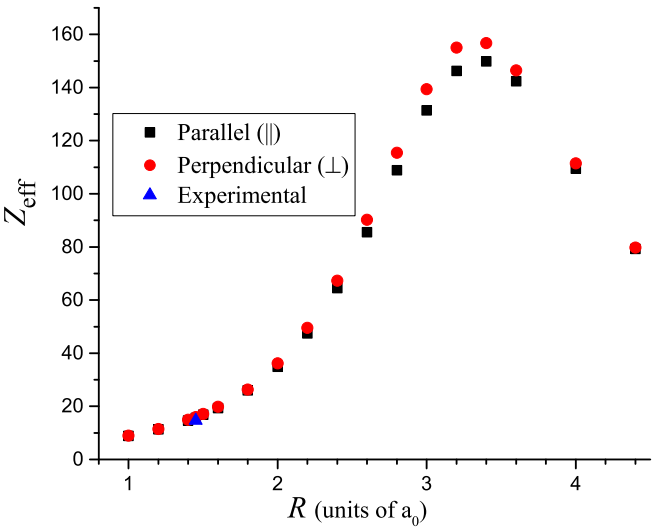

FIG. 4. (Color online) Annihilation parameter Z_{eff} as a function of the internuclear distance R for e^+-H_2 scattering. The experimental values are those from Table I.

and 14.61 [13] are included in Table I for comparison, showing reasonable agreement with the theoretical results. As pointed out earlier [32], the variation among the experimental values is probably related to different densities of the H_2 gas [8].

Figures 1 and 2 present for e^+-H_2 scattering the scattering length A_{scat} and annihilation parameter Z_{eff} as function of the angle θ_3, respectively, for different values of R. Due to the symmetry plane passing through the center-of-mass of the molecule perpendicular to the molecular axis, the values for θ_3 and $\pi - \theta_3$ are the same and we can restrict the plots to the range $0 \leqslant \theta_3 \leqslant \pi/2$. Corresponding plots of A_{scat} and Z_{eff} as a function of the internuclear distance R are given in Figs. 3 and 4, respectively, separately for $\theta_3 = 0$ and $\theta_3 = \pi/2$. The minimum in the scattering length around $R \approx 3.4a_0$ indicates the formation of a virtual state [32,46]. The effect of the polarization on the scattering length lies within a range of 1% to 5% for $1a_0 \leqslant R \leqslant 4a_0$. For $R = 1.4a_0$, for example, it is 3.0%. Since $A_{scat,\parallel}$ and $A_{scat,\perp}$ for the same R deviate by not more than 13% throughout all calculations, the near-zero energy e^+-H_2 scattering can be approximately described by a system of spherical symmetry.

B. Near-zero-energy electron scattering from H_2

Table II addresses the convergence of the calculations for the Σ_g e^--H_2 system for $R = 1.4a_0$ as a function of the number of ECGs. For an increasing number of short-range basis functions $A_{scat,\parallel}$ decreases while $A_{scat,\perp}$ increases monotonically. For low-energy electron scattering by nonpolar molecules, the total and diffusion cross sections can be approximately expressed as a function of the wave number k. The fitting parameters include the scattering length A_{scat}, which largely depends on the short-range interaction. By fitting the experimental diffusion cross sections of Crompton and co-workers [3], Chang found $A_{scat} = 1.27 \pm 0.01a_0$ [33,34]

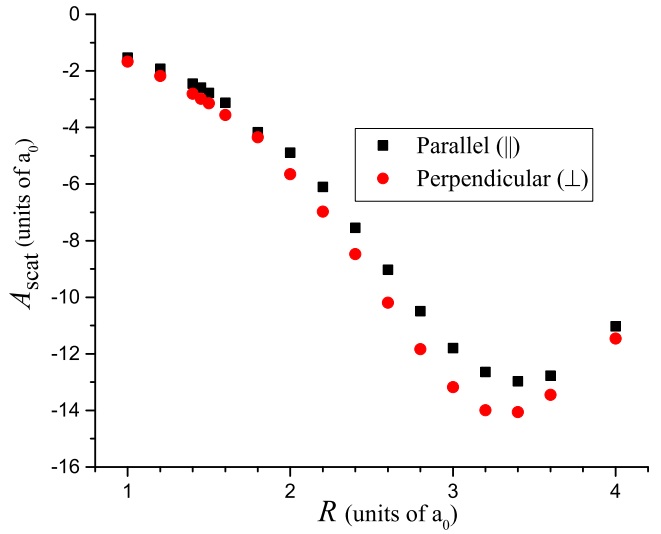

FIG. 3. (Color online) Scattering length A_{scat} as a function of the internuclear distance R for e^+-H_2 scattering.

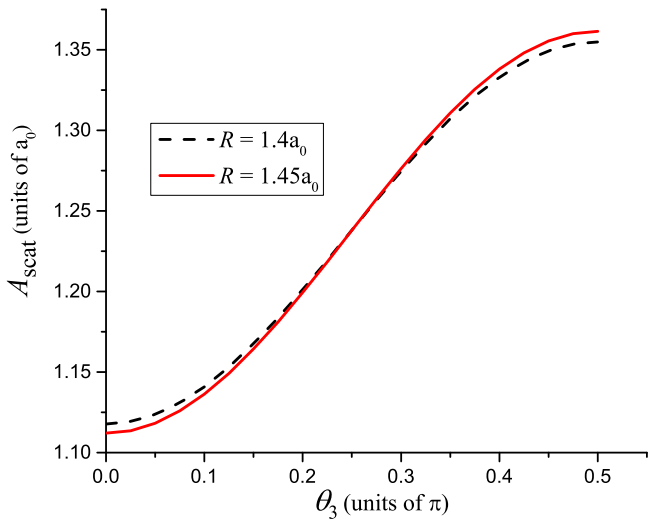

FIG. 5. (Color online) Scattering length A_{scat} as a function of the angle θ_3 for e^--H_2 scattering.

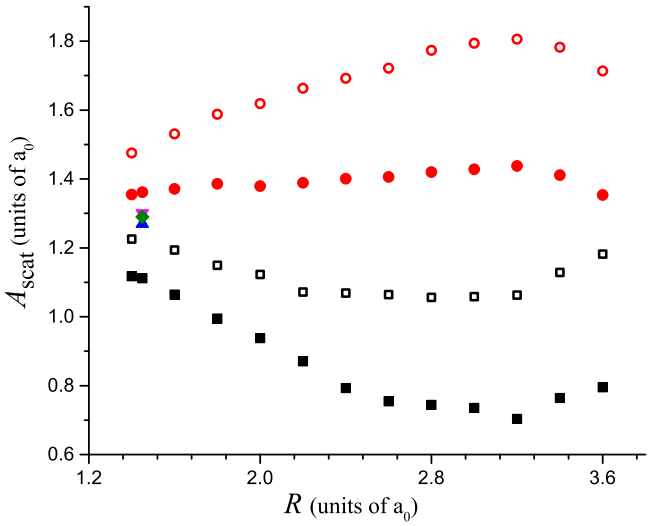

FIG. 6. (Color online) Scattering length A_{scat} as a function of the internuclear distance R for e^--H_2 scattering. Empty and filled circles: $A_{scat,\parallel}$ without and with polarization correction, respectively. Empty and filled squares: $A_{scat,\perp}$ without and with polarization correction, respectively. The triangle and diamond symbols refer to the references from Table II.

and Fabrikant estimated $A_{scat} = 1.29a_0$ [35]. The small difference is mainly due to the fact that Chang determined the isotropic part of the polarizability as $\alpha = 5.4 \pm 0.1a_0^3$, whereas Fabrikant used $\alpha = 5.18a_0^3$. Fedus and co-workers obtained $A_{scat} = 1.30a_0$ and $\alpha = 5.314a_0^3$ [47]. All three MERT values of A_{scat} are within the range of our $A_{scat,\parallel}$ and $A_{scat,\perp}$.

Figure 5 presents for e^--H_2 scattering the scattering length A_{scat} as a function of the angle θ_3. The difference between $R = 1.4$ and $1.45a_0$ is less than 0.5%, whereas for e^+-H_2 scattering this difference is about 6.0%. According to Fig. 5, the mean scattering length is $1.24a_0$, in agreement with the accurate MERT values within 3% to 4% [23,34,35]. Since the size of the optimized basis set for the e^+-H_2 system (1400) is much larger than that for the e^--H_2 system (1000), it is likely that the accuracy of our calculations in the former case is better than 4%. This indicates that the uncertainty of the experimental scattering lengths is large. Figure 6 gives $A_{scat,\parallel}$ and $A_{scat,\perp}$ as functions of the internuclear distance R. As compared to the e^+-H_2 scattering, the effect of polarization is much larger for the e^--H_2 scattering. The polarization correction lies within a range of 8% to 35% for $1.4a_0 \leqslant R \leqslant 3.6a_0$. For $R = 1.4a_0$, for example, it is 8.5%. Since the convergence is slower for $A_{scat,\parallel}$ than for $A_{scat,\perp}$ for each R when the number of basis functions increases, we expect that $A_{scat,\parallel}$ is less accurate, especially for large R. In addition, it is less accurate for large R than for small R. $A_{scat,\parallel}$ shows a tendency to decrease when R increases, reaching a minimum at $R = 3.2a_0$. On the other hand, $A_{scat,\perp}$ increases slightly for increasing R, with a maximum at $R = 3.2a_0$.

IV. CONCLUSION

To conclude, the near-zero-energy $e^{\pm}$-H_2 scattering has been studied by the stabilization method with ECGs. For e^+-H_2 scattering, the presented results are significantly more accurate than previous ECG calculations [32,40], as well as Kohn variational calculations [41,43]. The results of A_{scat} agree with MERT values. In addition, the obtained values for Z_{eff} are compatible with the experiment. In particular, the success of the e^+-H_2 calculations testifies the potential of merged basis sets for different distances R. This strategy also turnes out to be very useful for e^--H_2 scattering, as it avoids near-linear dependencies for increasing basis size. Our results represent a first principles determination of the scattering length without model potentials. The calculated mean scattering length at $R = 1.45a_0$ shows good agreement with MERT values [23,34,35].

ACKNOWLEDGMENTS

The authors are thankful for computational resources provided by KAUST HPC and ACEnet of Canada. Z.-C.Y. is supported by NSERC of Canada, by the Canadian computing facilities of SHARCnet and ACEnet, and in part by the Chinese Academy of Sciences CAS/SAFEA International Partnership Program for Creative Research Teams. Y.-J.Y. is supported by the National Magnetic Confinement Fusion Science Programme of China under Contracts No. 2011GB107001 and No. 2011GB107003.

[1] H. Ehrhardt, L. Langhans, F. Linder, and H. S. Taylor, Phys. Rev. **173**, 222 (1968).
[2] R. W. Crompton, M. T. Elford, and A. I. McIntosh, Aust. J. Phys. **21**, 43 (1968).
[3] R. W. Crompton, D. K. Gibson, and A. I. McIntosh, Aust. J. Phys. **22**, 715 (1969).
[4] F. Linder and H. Schmidt, Z. Naturforsch. A **26**, 1603 (1971).
[5] S. Hara, J. Phys. B **7**, 1748 (1974).
[6] A. Klonover and U. Kaldor, J. Phys. B **11**, 1623 (1978).
[7] J. D. McNutt, S. C. Sharma, and R. D. Brisbon, Phys. Rev. A **20**, 347 (1979).
[8] G. L. Wright, M. Charlton, G. Clark, T. C. Griffith, and G. R. Heyland, J. Phys. B **16**, 4065 (1983).
[9] E. A. G. Armour, J. Phys. B **17**, L375 (1984).
[10] E. A. G. Armour, J. Phys. B **18**, 3361 (1985).
[11] E. A. G. Armour and D. J. Baker, J. Phys. B **18**, L845 (1985).
[12] E. A. G. Armour and D. J. Baker, J. Phys. B **19**, L871 (1986).
[13] G. Laricchia, M. Charlton, C. D. Beling, and T. C. Griffith, J. Phys. B **20**, 1865 (1987).
[14] M. A. Khakoo, S. Trajmar, R. McAdams, and T. W. Shyn, Phys. Rev. A **35**, 2832 (1987).
[15] Z. Lj. Petrović and R. W. Crompton, Aust. J. Phys. **40**, 347 (1987).
[16] M. A. Morrison, R. W. Crompton, B. C. Saha, and Z. Lj. Petrović, Aust. J. Phys. **40**, 239 (1987).
[17] J. P. England, M. T. Elford, and R. W. Crompton, Aust. J. Phys. **41**, 573 (1988).
[18] S. J. Buckman, M. J. Brunger, D. S. Newman, G. Snitchler, S. Alston, D. W. Norcross, M. A. Morrison, B. C. Saha, G. Danby, and W. K. Trail, Phys. Rev. Lett. **65**, 3253 (1990).

[19] M. J. Brunger, H. Cho, H. Tanaka, and S. J. Buckman, J. Phys. B **24**, 1435 (1991).
[20] S. D. Sanchez and M. A. P. Lima, Nucl. Instrum. Methods, Phys. Res. B **266**, 447 (2008).
[21] A. Zecca, L. Chiari, A. Sarkar, K. L. Nixon, and M. J. Brunger, Phys. Rev. A **80**, 032702 (2009).
[22] L. Phan Thi and J. Byung-Hoon, J. Phys. Soc. Jpn. **81**, 104501 (2012).
[23] K. Fedus, G. P. Karwasz, and Z. Idziaszek, Phys. Rev. A **88**, 012704 (2013).
[24] F. E. Harris, Phys. Rev. Lett. **19**, 173 (1967).
[25] R. J. Drachman and S. K. Houston, Phys. Rev. A **12**, 885 (1975).
[26] S. F. Boys, Proc. R. Soc. A **258**, 402 (1960).
[27] K. Singer, Proc. R. Soc. A **258**, 412 (1960).
[28] Y. Suzuki and K. Varga, *Stochastic Variational Approach to Quantum-Mechanical Few-Body Problems* (Springer, New York, 1998).
[29] J. Y. Zhang and J. Mitroy, Phys. Rev. A **78**, 012703 (2008).
[30] J. Y. Zhang, J. Mitroy, and K. Varga, Phys. Rev. A **78**, 042705 (2008).
[31] J. Mitroy, J. Y. Zhang, and K. Varga, Phys. Rev. Lett. **101**, 123201 (2008).
[32] J.-Y. Zhang, J. Mitroy, and K. Varga, Phys. Rev. Lett. **103**, 223202 (2009).
[33] E. S. Chang, Phys. Rev. A **9**, 1644 (1974).
[34] E. S. Chang, J. Phys. B **14**, 893 (1981).
[35] I. I. Fabrikant, J. Phys. B **17**, 4223 (1984).
[36] V. I. Kukulin and V. M. Krasnopol'sky, J. Phys. G **3**, 795 (1977).
[37] K. Varga and Y. Suzuki, Phys. Rev. C **52**, 2885 (1995).
[38] W. Cencek and K. Szalewicz, Int. J. Quantum Chem. **108**, 2191 (2008).
[39] A. M. Arthurs and A. Dalgarno, Proc. R. Soc. A **256**, 540 (1960).
[40] J. Y. Zhang and J. Mitroy, Phys. Rev. A **83**, 022711 (2011).
[41] E. A. G. Armour, J. N. Cooper, M. R. Gregory, S. Jonsell, and M. Plummer, J. Phys. Conf. Ser. **199**, 012007 (2010).
[42] J. N. Cooper, Ph.D. thesis, University of Nottingham, UK, 2009.
[43] J. N. Cooper, E. A. G. Armour, and M. Plummer, J. Phys. A **42**, 095207 (2009).
[44] K. R. Hoffman, M. S. Dababneh, Y.-F. Hsieh, W. E. Kauppila, V. Pol, J. H. Smart, and T. S. Stein, Phys. Rev. A **25**, 1393 (1982).
[45] G. P. Karwasz, D. Pliszka, and R. S. Brusa, Nucl. Instrum. Methods, Phys. Res. B **247**, 68 (2006).
[46] E. A. G. Armour, Phys. Rev. A **82**, 042702 (2010).
[47] T. N. Olney, N. Cann, G. Cooper, and C. Brion, Chem. Phys. **223**, 59 (1997).
[48] E. A. G. Armour, J. Phys. Conf. Ser. **225**, 012002 (2010).